DESIGN OF CFRP STIFFENED PANELS BY PFA

F. Romano[1], F. Di Caprio[2], U. Mercurio[3] and L. Lecce[4]

[1]Aeronautics - Technologies Integration, CIRA, Via Maiorise snc 81043 Capua (CE), Italy
Email: f.romano@cira.it, Web Page: http://www.cira.it
[2]Aerostructural Design and Dynamic, CIRA, Via Maiorise snc 81043 Capua (CE), Italy
Email: f.dicaprio@cira.it, Web Page: http://www.cira.it
[3]Aeronautics - Engineering of Aeronautical Systems, Via Maiorise snc 81043 Capua (CE), Italy
Email: u.mercurio@cira.it, Web Page: http://www.cira.it
[4]Dept. of Industrial Engineering, Univ. of Naples "Federico II", Via Claudio 21 80125 Napoli, Italy
Email: leonardo.lecce@unina.it, Web Page: http://www.unina.it

Keywords: composites, PFA, residual strength

Abstract

The object of this work is the evaluation of the collapse load of stiffened CFRP wing panels by applying progressive failure analysis methodology (PFA). The aim is to show the effectiveness of this methodology to predict the real mechanical behaviour of the panels in presence of discrete damages, against the traditional design approach.

The PFA has been performed on a stiffened panel, loaded in compression, representative of the upper surface, at the wing root, of a typical regional aircraft wing box. Holes 1/4 inch (6.35 mm) in diameter have been applied in the skin of the panel, as representative in a preliminary design phase of low energy impact damages. Different hole scenarios have been considered in order to give useful indications about the sensitivity of the residual strength of the panel respect to the densities of damages and different damage locations. Significant potential weight reduction and higher residual strength have been found respect to the traditional design. These results will be useful tools to support in the future new design approaches at element level (stiffened panel), or to design with a reduced allowable for damage higher respect to that one obtained by CAI (Compression After Impact) tests on coupon.

1. Introduction

The use of composite materials is very attractive because of their outstanding strength, stiffness, and light-weight properties. Composite materials have been increasingly used in civil aviation over the last three decades. But, due to the high sensitivity to damage and defects, in particular low energy impact damage, the full potential of composite materials is not exploited resulting in increased structural mass. In order to predict the full potential of aircraft composite structures, is essential to use reliable methodologies that overcome the current failure design approach that is based on the first ply failure criteria, aiming at predicting the effective collapse load of a composite structure taking into account the propagation and/or accumulation of initial local failures. The traditional design approach of these structures is based on the use of the material design values degraded for low energy impact damage using results obtained at coupon level: the whole stiffened panel is considered uniformly damaged instead of considering a discrete damage model.

The structural substantiation for BVID (Barely Visible Impact Damage) includes demonstration of a reliable service life, while retaining ultimate design load [1]. The catastrophic failure of a composite structure, i.e. its ultimate load-carrying capability, rarely occurs at the load corresponding to the first-

Excerpt from ISBN 978-3-00-053387-7

ply failure (FPF). Composite structures usually fail due to the propagation or accumulation of local failures as the load is increased.
During the years, new advanced numerical methodologies, named Progressive Failure Analysis (PFA), based on the Finite Element Method (FEM), have been developed and employed in order to simulate the real capability of composite structures: in addition to the damage initiation (FPF), also the damage propagation up to the collapse load of the structure [2–8]. The present work shows the results obtained by simulating the progressive damage of a complex structure: a damaged stiffened panel under compressive load; the panel is sized at strength, and it is representative of the upper skin panel, toward the wing root, of the wing box of a typical Regional Aircraft. Discrete barely visible impact damages have been introduced in the FE model of the panel.
Generally, in order to determine the strength of an impacted panel it is mandatory to simulate, at first, the impact event, and then the compression test. The numerical analyses of impact event are very expensive; this is the reason for what this kind of analyses are avoided in the preliminary design phase, and simplified damage models are commonly used. According to some industrial design guidelines [9, 10], in the preliminary design phase it is possible to consider the degradation of the strength due to a BVID with that one due to a hole 1/4 in. (6.35 mm) in diameter; hereafter the BVID is considered equivalent to a hole and it will be called simply discrete damage. According to this method, different locations of a discrete damage in the skin of the stiffened panel have been analysed in this work, and also different multi-damage maps have been considered as representative of more realistic damage scenarios.
The PFA performed on the panel has been finalized to evaluate the sensitivity of the residual strength of the panel to different damage locations and damage density. For the research objectives of the present work, the panel has been considered flat; discrete damages only in the skin of the panel have been analysed, and no delaminations and disbonding skin-stringers have been considered. In a future research activity it is foreseen to analyse the panel behaviour in presence of delaminations and skin-stringer disbondings.

2. Panel description

The stiffened panel consists of a flat, rectangular graphite–epoxy panel with six T shaped stringers; Fig. 1 illustrates the panel geometry and the boundary conditions. The panel is loaded in axial compression: a uniform displacement along the y-axis is applied to the edge AB, U_y=U_0. The stacking sequence of the skin, cap and web of the stringers, are shown in Table 1. The material is a unidirectional CFRP (Carbon Fiber Reinforced Plastic) prepreg tape, commonly used for aeronautical applications. The mechanical properties of the unidirectional lamina are summarized in Table 2. The lamina strength properties shown in this table are degraded by appropriate knockdown factors to take into account their decrease due to B-basis statistical reduction, temperature and moisture effects.
This panel is the result of the current traditional design approach, based on the FPF criteria, and on the assumption that the panel is wholly damaged; the latter is simulated by applying a knockdown factor for BVID, K_{BVID}, to the pristine material strength properties, in addition to the other above knockdown factors. The factor K_{BVID} is generally evaluated by means of CAI (Compression After Impact) tests, and its value is about 0.4, thus the material strength properties are further reduced up to 60%. The final compressive allowable of this material, based also on the application of the BVID knockdown factor, is resulted equal to 2120 $\mu\varepsilon$. It is evident that this design approach can lead to oversized structures.
The panel with the lamina material properties of Table 2 (no K_{BVID} application) and without discrete damages, is called in this work with the acronym UDA (undamaged). The finite element model of the UDA panel is shown in Fig. 2. The entire panel is discretized by means of four-node layered shell element with a full integration scheme. The linkage between the skin and the stringers is modelled by contact elements with multi-point constraints option.

Excerpt from ISBN 978-3-00-053387-7

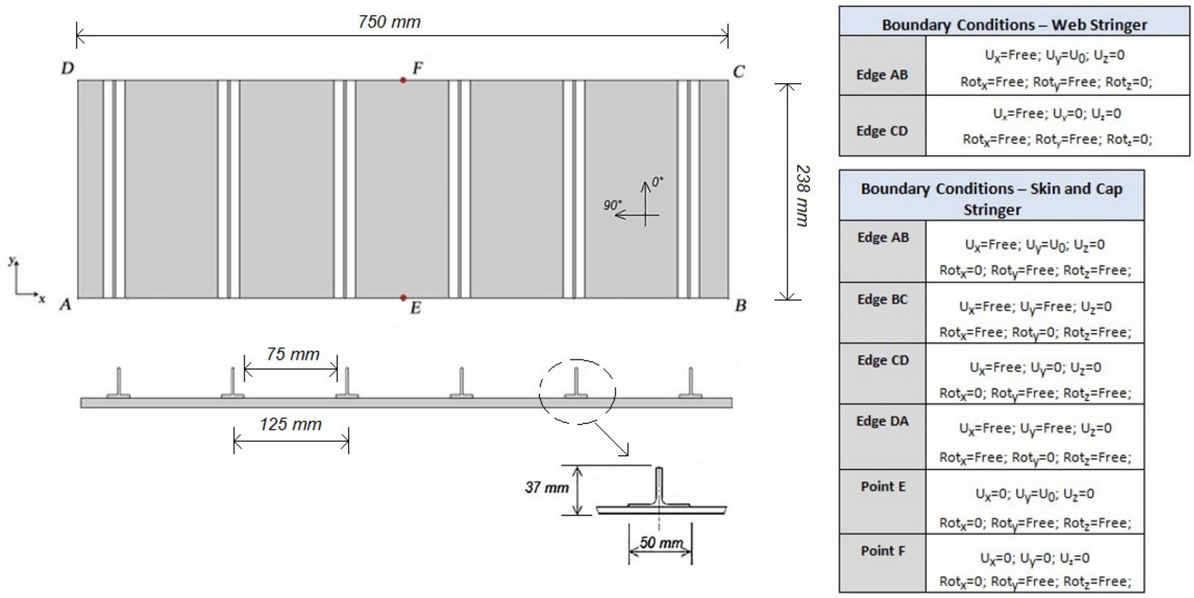

Figure 1. Geometry and boundary conditions.

Table 1. Laminates of the panel.

	No. plies	Layup
Skin	28	[45/-45/45/-45/0/0/90/0/0/45/-45/0/90/0]s
Cap-Stringer	12	[45/-45/0/0/90/0]s
Web-Stringer	24	[45/-45/0/0/90/0/0/90/0/0/-45/45]s

Table 2. Lamina material properties.

Ply thickness	t_{ply}	0.186	mm
Density	ρ	1600	Kg/m^3
Longitudinal Young's modulus	E_1	150	GPa
Transverse Young's modulus	E_2	8.20	GPa
In-plane Shear modulus	G_{12}=G_{13}	3.95	GPa
Out-of-plane shear modulus	G_{23}	2.52	GPa
Poisson's ratio	ν_{12}, ν_{13}	0.35	
Longitudinal Tensile Strength	F_{1t}	1764	MPa
Longitudinal Tensile Strain	ε_{1t}	10825	$\mu\varepsilon$
Longitudinal Compressive Strength	F_{1c}	740	MPa
Longitudinal Compressive Strain	ε_{1c}	5383	$\mu\varepsilon$
Transverse Tensile Strength	F_{2t}	56	MPa
Transverse Tensile Strain	ε_{2t}	6795	$\mu\varepsilon$
Transverse Compressive Strength	F_{2c}	170	MPa
Transverse Compressive Strain	ε_{2c}	20750	$\mu\varepsilon$
Shear Strength	F_{12}	66	MPa
Shear Strain	γ_{12}	16792	$\mu\varepsilon$

Excerpt from ISBN 978-3-00-053387-7

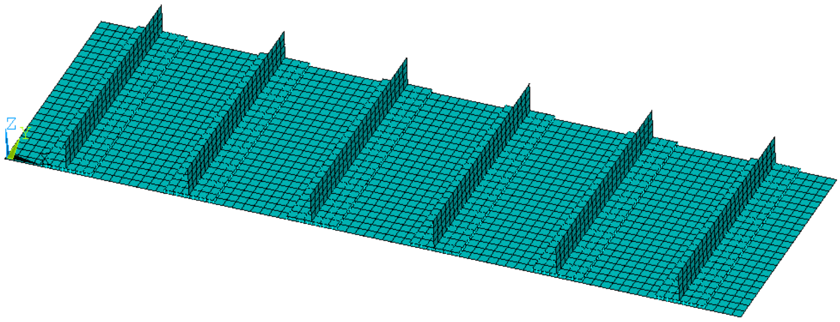

Figure 2. UDA panel: finite element model.

3. PFA methodology

The Progressive Failure Analysis methodology is finalised to predict failure initiation and propagation in composite laminated structures. The PFA is based on non-linear analysis [4]. At each load step, a non-linear analysis is performed until a converged solution is obtained. Then, using this equilibrium state, the stress distribution in each lamina is computed and stored. The stresses are introduced into specified failure criteria, which are then checked to determine whether any failures have occurred or not. If the adopted failure criterion indicates that lamina failure has occurred, the elastic lamina properties are degraded according to a particular degradation model. Since the initial nonlinear solution no longer corresponds to an equilibrium state due to the fact that the material properties have been degraded, equilibrium of the structures needs to be re-established utilizing the modified lamina properties for the failed lamina while keeping the current load level. This iterative process, of obtaining nonlinear equilibrium solutions each time a local material model is changed, is continued until no additional lamina failures are found. The load step is then incremented until catastrophic failure of the structure is detected, i.e. converged solution is no more obtained. PFA is therefore based on the selection of the type of the failure criterion utilized to evaluate the failure initiation and the material degradation model implemented to decrease the load carrying capability of the damaged structure. In this work Hashin criteria [11] has been selected as lamina failure criteria, in order to evaluate separately fibre failure and matrix failure (tensile fiber, compressive fiber, tensile matrix and compressive matrix), and the instantaneous unloading degradation model: the stiffness material property associated with that mode of failure, E_j, is degraded instantly to a fraction K of the initial value:

$$E_{j\_new} = K\, E_{j\_old}. \tag{1}$$

In this work the PFA has been carried out in MSC Nastran® by using SOL 400 solution process [12].

4. Discrete damage model analysis

In order to evaluate the real capability of the stiffened panel, discrete damages have been introduced in the panel and keeping the mechanical strength properties of the material without degradation for BVID. For this purpose, according to the simplified design approach, in particular to the indications enclosed in the guideline for the preliminary design of composite structures issued by Northrop Grumman [10], a hole 6.35 mm (1/4 in.) in diameter has been used as equivalent to the BVID. Different locations of a discrete damage in the skin have been analysed, and also multi-damage maps have been considered, to fully investigate the sensitivity of the total failure of the panel, i.e. collapse load, with respect to different damage scenarios. In the latter case maps with three, five, and seven holes have been considered. Fig. 3 illustrates a scheme of different locations of the holes in the skin and the relative identification code. In particular the main locations of the single hole in the skin are:

Excerpt from ISBN 978-3-00-053387-7

in the middle of a stringer bay (1Ha), at the edge of the cap of the stringer (1Hb), under the cap of the stringer (1Hc), very close to the cap of the stringer (1Hd). The multi-hole maps, with 3, 5 and 7 holes are a combination of the above mentioned cases with a single hole.

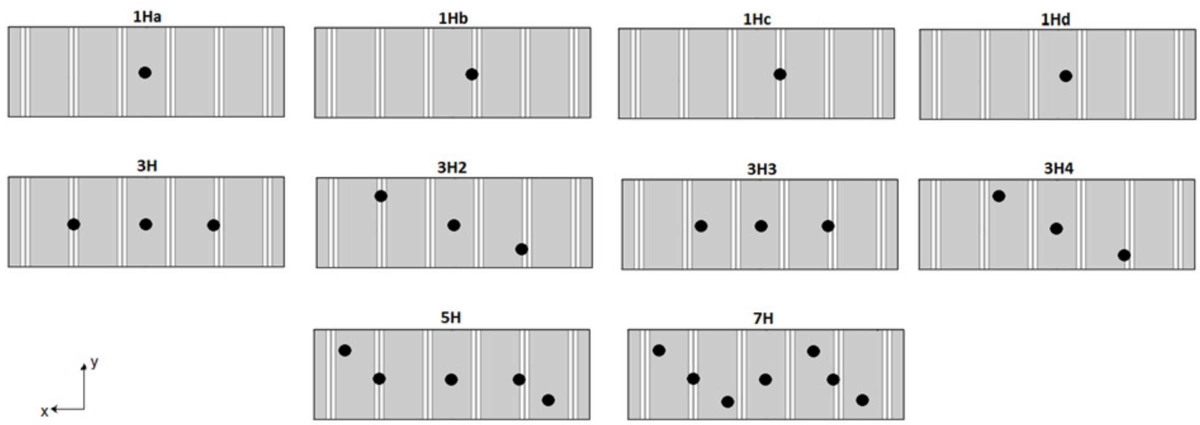

Figure 3. Damage scenarios.

4.1. PFA results for the panels with one hole

The presence of the damage triggers off the degradation of the material inducing a propagation of the damage from the initiation of the failure in a lamina, FPF load, up to the total failure of the panel, TF load (Fig. 4). As expected, the failure of the panel starts close to the hole and it propagates along a line perpendicular to the load direction. FPF load and TF load are not coincident (Fig. 5, Table 3) as instead happens for the UDA panel (i.e. without hole). The damaged ply is resulted the fifth one of the skin laminate, oriented at 0° and characterized by compressive fiber failure.
Obviously all the hole locations anticipates the TF load respect to the UDA panel of at least 33%, for the least critical case 1Hc, up to 38% for the most critical case 1Hb. In terms of FPF and TF load, the hole under the cap of the stringer (1Hc) is the least critical location; the most critical location in terms of FPF is obtained with the hole 1Ha (in the middle of the stringer bay); the total failure reaches its lowest value with the hole at the edge of the cap of the stringer (1Hb), in particular it is lower of about 8% than the least critical case 1Hc (in this case the cap of the stringer performs the function of a sort of bridge for the load).

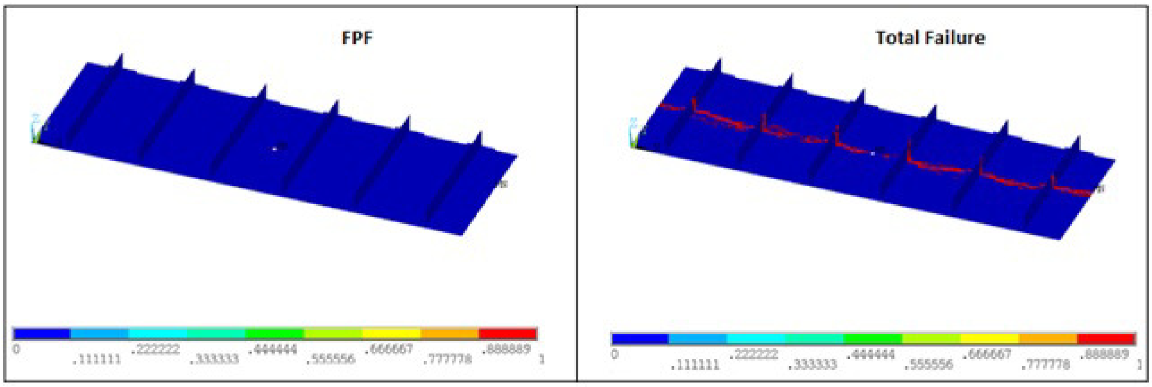

Figure 4. Progressive failure of the panel with one hole in the middle of the stringer bay.

Excerpt from ISBN 978-3-00-053387-7

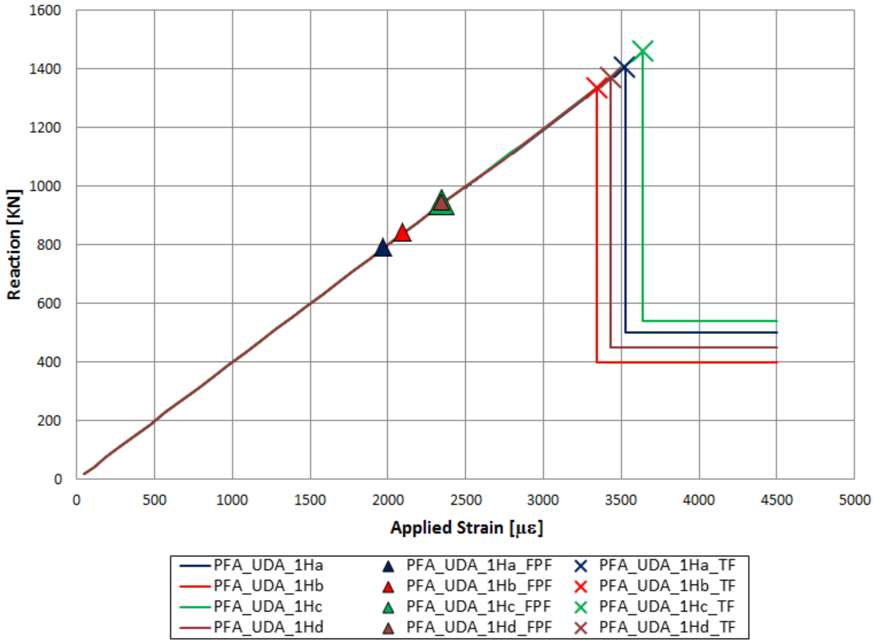

Figure 5. Reaction vs Applied Strain – panels with all the hole locations 1H.

Table 3. Panels with one hole: FPF and Total Failure.

	FPF load (kN)	%	FPF strain (με)	%	Total Failure (kN)	%	Failure strain (με)	%
PFA_UDA_1Hc	944	-	2343	-	1458	-	3639	-
PFA_UDA_1Ha	793	-16	1966	-16	1406	-3.5	3525	-3
PFA_UDA_1Hd	944	0	2343	0	1370	-6	3433	-6
PFA_UDA_1Hb	843	-11	2092	-11	1335	-8	3346	-8

4.2. PFA results for the panels with multi-hole maps

Fig. 6 and Table 4 summarize the PFA results obtained for the multi-hole maps. Obviously all the multi-hole maps anticipate the TF load respect to the panels with one hole, also up to a reduction of about 15%. As expected, the panels 5H and 7H have a lower collapse load respect to the panels with 3 holes. The residual strength of the panel with seven holes, 7H, is practically coincident with that one of the panel with five holes, 5H: 1240 kN of the panel 7H against 1252 kN of the panel 5H, with a difference of only 1%. Fig. 7 shows the damaged elements at the collapse point of the panel 5H.

4.3. Resume of the PFA results and design implications

Table 5 summarizes the comparison between the most critical values of each damage scenario (1 hole, 3 holes, 5 holes, 7 holes). A damage scenario with five holes is practically sufficient to completely exhaust the residual strength of the stiffened panel (§ 4.2). In particular, even if a limited number of holes completely exhausts the residual strength of the panel, on the other hand the compressive failure strain (3131 με, five holes) is higher than the design allowable obtained at coupon level by CAI tests, 2120 με, and used in the traditional design approach. The compressive failure strain of 3131 με, that represents the actual residual strength of the panel according to the results of the PFA performed on

Excerpt from ISBN 978-3-00-053387-7

the panel with discrete damages, could allow to design a lighter panel and/or a panel with higher load carrying capability with respect to the panel obtained by the traditional design.

A measure of the weight reduction achievable can be appreciated considering that the stiffened panel shown in § 2, that has been sized using the traditional compressive design allowable based on BVID degradation factor (2120 με), if redesigned for the same design load capability, but using as design value 3131 με, should have a weight lower of about 30%.

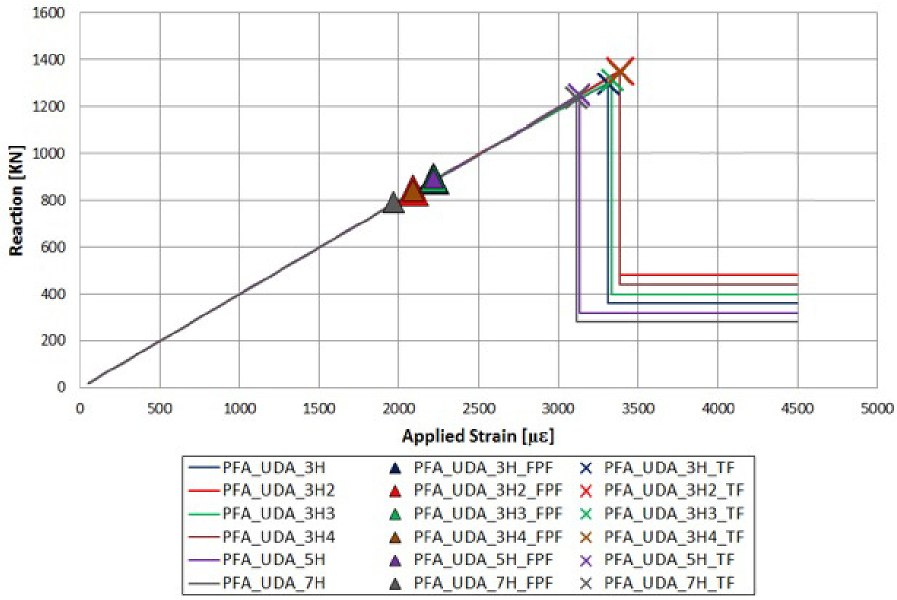

Figure 6. Reaction vs Applied Strain – panels with 3, 5 and 7 holes.

Table 4. Panels with 3, 5 and 7 holes: FPF and Total Failure.

	FPF load (kN)	%	FPF strain (με)	%	Total Failure (kN)	%	Failure strain (με)	%
PFA_UDA_3H2	842	-	2092	-	1330	-	3340	-
PFA_UDA_3H4	842	0	2092	0	1320	-1	3340	0
PFA_UDA_3H3	893	6	2217	6	1312	-1	3338	0
PFA_UDA_3H	893	6	2217	6	1299	-2	3312	-1
PFA_UDA_5H	892	6	2217	6	1252	-6	3131	-6
PFA_UDA_7H	791	-6	1966	-6	1240	-7	3115	-7

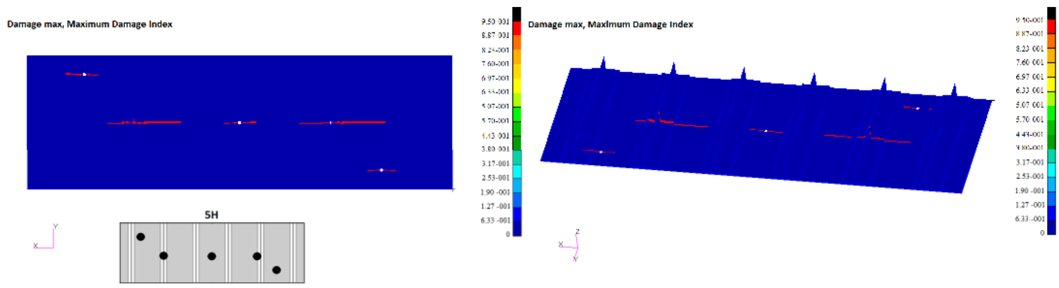

Figure 7. Collapse of the panel 5H.

Excerpt from ISBN 978-3-00-053387-7

Table 5. Comparison between the most critical values of the Total Failure load.

1 hole	-38%	*vs* UDA						
3 holes	-40%	*vs* UDA	-3%	*vs* 1 hole				
5 holes	-42%	*vs* UDA	-6%	*vs* 1 hole	-3.6%	*vs* 3 holes		
7 holes	-43%	*vs* UDA	-7%	*vs* 1 hole	-4.5%	*vs* 3 holes	-1%	*vs* 5 holes

5. Conclusions

The progressive failure analysis performed on the stiffened panel presented in this work, has shown the sensitivity of the final failure load of the panel to different damage scenarios. Both a single hole, positioned in different locations, and maps of three, five and seven holes have been considered. The results of PFA have shown the sensitivity of the collapse load to the hole location. The total failure of the panel decreases with the increasing of the number of the holes up to the panel with five holes; for the latter, the total failure is practically the same of that one with seven holes. Consequently the damage scenario with five holes is sufficient to completely exhaust the residual strength of the panel. This result gives useful indications in terms of the real capability to take into account in the design of the stiffened panel, providing useful guidelines in terms of the real design value in compression to be considered in the design of the panel respect to the traditional one. In the latter case the design can lead to a not efficient structure in terms of weight and/or load carrying capability with respect to considering the actual residual strength of the panel according to the results of the PFA performed on the panel with discrete damages. This paper has shown the effectiveness of the PFA as design tool to investigate a new design methodology by evaluating the capability of the panel in presence of discrete maps of damages, up to detect that one that is able to exhaust the strength of the panel.

References

[1] EASA AMC 20–29. Composite aircraft structure. 2010.
[2] H. Suemasu, H. Takahashi, T. Ishikawa. On the failure mechanisms of composite laminates with an open hole subjected to compressive load. *Composite Science and Technology*, 66:634–41, 2006.
[3] I. Lapczyk, J.A. Hurtado. Progressive damage modeling in fiber-reinforced materials. *Composites Part A*, 38:2333–41, 2007.
[4] D.W. Sleight. Progressive failure analysis methodology for laminated composite structures. *NASA Technical Paper*, NASA/TP-1999-209107, 1999.
[5] C. Schuecker, H.E. Pettermann. Constitutive ply damage modeling, FEM implementation, and analyses of laminated structures. *Computers & Structures*, 86:908–18, 2008.
[6] R. Borrelli, F. Di Caprio, U. Mercurio, F. Romano. Assessment of progressive failure analysis capabilities of commercial FE codes. *International Journal of Structural Integrity*, 4(3):300–20, 2013.
[7] R. Borrelli, S. Franchitti, F. Di Caprio, F. Romano, U. Mercurio. A numerical procedure for the virtual compression after impact analysis. *Advanced Composites Letters*, 24(4):57-67, 2015.
[8] F. Romano, F. Di Caprio, B. Auriemma, U. Mercurio. Numerical investigation on the failure phenomena of stiffened composite panels in post-buckling regime with discrete damages. *Journal of Engineering Failure Analysis*, 56:116-130, 2015.
[9] C. Kassapoglou. *Design and analysis of composite structures with applications to aerospace structures*. John Wiley & Sons, 2010.
[10] J.A. Bailie, R.P. Ley, A. Pasricha. A summary and review of composite laminate design guidelines. Northrop Grumman Report under NASA Contract NAS1-19347, 1997.
[11] Z. Hashin. Failure criteria for unidirectional fiber composites. *Journal of Applied Mechanics*, 47:329–34, 1980.
[12] MSC Nastran®. MSC Nastran quick reference guide. 2014.

Excerpt from ISBN 978-3-00-053387-7